

Research Article

A Novel Cellular Handset Design for an Enhanced Antenna Performance and a Reduced SAR in the Human Head

Salah I. Al-Mously^{1,2} and Marai M. Abousetta^{1,2}

¹ Department of Electrical and Electronics Engineering, School of Applied Sciences and Engineering, Academy of Graduate Studies, P.O. Box 79031, Janzoor, Tripoli, Libya

² Department of Microwave and Radar Engineering, The Higher Institute of Electronics, P.O. Box 38645, Beni-Walid, Libya

Correspondence should be addressed to Salah I. Al-Mously, salah.mously@hieb.edu.ly

Received 17 November 2007; Accepted 21 March 2008

Recommended by Seong-Youp Suh

This paper presents a novel cellular handset design with a bottom-mounted short loaded-whip antenna. This new handset design is modeled and simulated using a finite difference time-domain (FDTD)-based platform *SEMCAD*. The proposed handset is based on a current commercially available bar-phone type with a curvature shape, keypad positioned above the screen, and top-mounted antenna. The specific absorption rates (SARs) are determined computationally in the specific anthropomorphic mannequin (SAM) and anatomically correct model of a human head when exposed to the EM-field radiation of the proposed cellular handset and the handset with top-mounted antenna. The two cellular handsets are simulated to operate at both GSM standards, 900 MHz as well as 1800 MHz, having different antenna dimensions and input power of 0.6 W and 0.125 W, respectively. The proposed human hand holding the two handset models is a semirealistic hand model consists of three tissues: skin, muscle, and bone. The simulations are conducted with handset positions based on the IEEE standard 1528-2003. The results show that the proposed handset has a significant improvement of antenna efficiency when it is hand-held close to head, as compared with the handset of top-mounted antenna. Also, the results show that a significant reduction of the induced SAR in the human head-tissues can be achieved with the proposed handset.

Copyright © 2008 S. I. Al-Mously and M. M. Abousetta. This is an open access article distributed under the Creative Commons Attribution License, which permits unrestricted use, distribution, and reproduction in any medium, provided the original work is properly cited.

1. INTRODUCTION

Due to enormous increase in the number of cellular handset users around the world, many questions are raised about the possible hazard effect of the cellular handset electromagnetic field (EMF) radiation. Thereby, health concerns regarding the use of a cellular handset near the human head have been growing and took a lot of attention by researchers.

The interaction of the cellular handset with the human head has been investigated by many published papers with considering; first, the effect of the human head on the handset antenna performance, including the feed-point impedance, gain, and efficiency [1–4], second, the impact of the antenna EM radiation on the user's head due to the absorbed power, which is measured by predicting the induced specific absorption rate (SAR) in head tissues [5, 6].

The protocol and procedures for the measurement of the peak spatial-average SAR induced inside a simplified head model of the cellular handset users are specified by

IEEE Standard-1528 [7] and IEC 62209-1 [8]. Both standards specified the specific anthropomorphic mannequin (SAM) as a simplified physical model (phantom) of the human head. This SAM has also been adopted by many committees, associations, and commissions [9–11]. The SAM has been developed by the IEEE Standards Coordinating Committee 34, Subcommittee 2, Working Group 1 (SCC34/SC2/WG1) as a lossless plastic shell, filled with a homogeneous liquid, and a thin lossless ear spacer, whereas (SCC34/SC2/WG2) has suggested the same SAM but with different plastic shell parameters [5].

Anatomically correct models of a nonhomogeneous human head at different ages were used to evaluate the performance of the handset on a human-head phantom [5, 12, 13]. In this paper, a nonhomogeneous high-resolution numerical correct model of a *European female head* [14], available with SPEAGE-Schmidt & Partner Engineering AG [15], is used.

Handset models with a keypad positioned above the screen are available commercially. Linux released a more comfortable of such a handset with a top-mounted external antenna and a curvature shape [16]. This new design ensures that much of the handset rests in the palm of the hand, thus, improving support and control. In addition to the improved grip, the thumb rests in a comfortable position directly above the buttons of the keypad. The improved angle for the thumb makes it unnecessary to shift the handset around in the hand while typing text [16].

In this paper, the proposed handset design with a bottom-mounted antenna is based on the handset model in [16]. An FDTD-based platform *SEMCAD* [15] is used for simulation. The Antenna performance is evaluated for both handset models in free space, hand-held, and hand-held close to head. A semirealistic hand model consists of three tissues is designed to simulate the human hand. The induced SAR's in head models are evaluated at GSM standards, 900 MHz and 1800 MHz, with antenna input power of 0.6 W and 0.125 W, respectively. Handset positions, *cheek* and *tilt* (15°), with respect to head are adopted according to IEEE standard 1528 [7].

2. CELLULAR HANDSET DESIGN AND FDTD SIMULATION

2.1. Handset structure

The handset model in [16] (will be referred later as model no. 1) is simulated using an FDTD-based platform *SEMCAD* (Simulation Platform for Electromagnetic Compatibility, Antenna Design and Dosimetry) ver. 12 *JUNGFRAU* [15]. The proposed handset with a bottom-mounted antenna (will be referred later as model no. 2) is also designed and simulated, where most handset components, such as PCB, LCD, Battery, and keypad, are considered in the design simulation. These components are not located identically in both handset models due to different antenna positions. Both models are simulated to operate at 900 MHz as well as 1800 MHz.

Figure 1(a) shows the physical model of the handset released by Linux [16], whereas Figure 1(b) exhibits the proposed physical model with bottom-mounted antenna. Figure 2 shows the numerical equivalent of both physical models used for the FDTD simulation. The maximum dimensions of both handsets are set to $45 \times 16 \times 130$ mm with a PCB symmetrically embedded inside the housing. The acoustic output position is set according to IEEE standard 1528 [7]. Figure 3 shows the numerical components structure of the handset models. The dielectric parameters of handset materials given in [6] are used.

2.2. Antenna design and specifications

Instead of using a helical antenna, a short-whip antenna top loaded with a small cylinder [17] is suggested for both designs of models as depicted in Figure 4. Table 1 shows the physical and electrical antenna specifications that optimized at both GSM standards for both handset models.



FIGURE 1: The physical model of (a) the handset released by Linux, and (b) the proposed handset with bottom-mounted antenna.

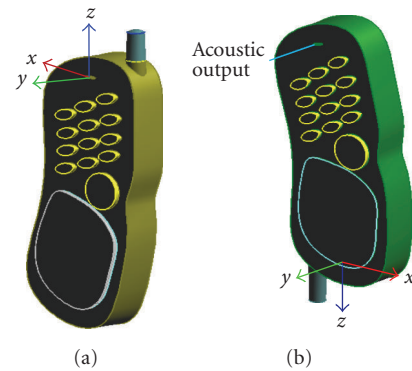


FIGURE 2: The CAD representation of both handset models.

3. GRID GENERATION AND SIMULATION FACTORS SETTING

3.1. Cellular handset in free-space

To align the simulated handset components to the FDTD grid accurately, a minimum spatial resolution of $0.1 \times 0.1 \times 0.1$ mm³ and maximum spatial resolution of $5 \times 5 \times 5$ mm³ in the x , y , and z directions are chosen with grading ratio of 1.2. For the handset model no. 1, the mesh cells amounts are 4.58979 Mcells and 3.95494 Mcells, at 900 MHz and 1800 MHz, respectively, whereas for the model no. 2, the mesh cells amounts are 6.82675 Mcells and 4.89154 Mcells, at 900 MHz and 1800 MHz, respectively.

3.2. Cellular handset in hand

A semirealistic human-hand model consists of three tissues: skin, muscle, and bone, are designed using *SEMCAD* [15] to simulate both handset models in hand, as shown in Figure 5. The FDTD grid has a minimum spatial resolution of $0.5 \times 0.5 \times 0.5$ mm³ and maximum spatial resolution of $10 \times 10 \times 10$ mm³ in the x , y , and z directions, with grading ratio of 1.2. For the hand-held of model no. 1, the mesh cells amounts are 4.58979 Mcells and 3.95494 Mcells, at 900 MHz and 1800 MHz, respectively, whereas for the hand-held of

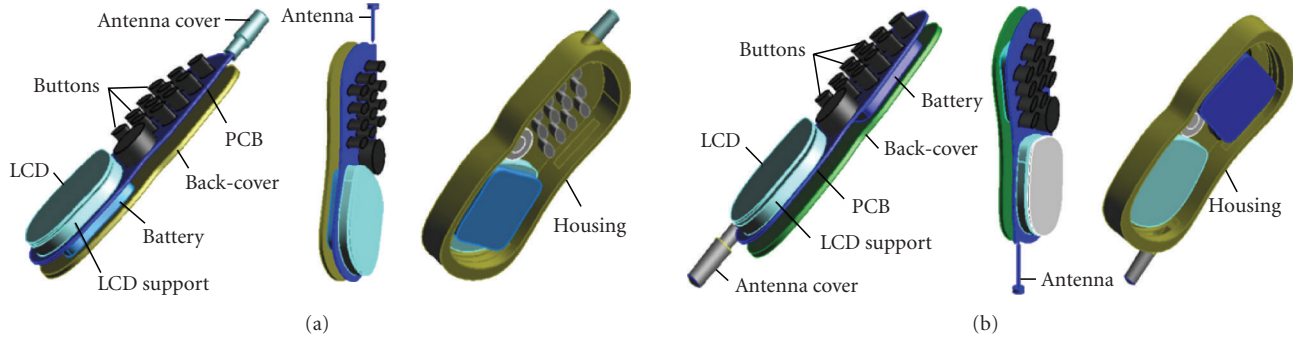


FIGURE 3: Numerical components structure of (a) the handset model no. 1, and (b) the proposed handset model no. 2.

TABLE 1: The proposed antenna dimensions and specifications for both handset design models at different frequencies.

<i>Model no. 1</i>						
Frequency	Matching lumped element	L_1	D_1	L_2	D_2	Impedance in ohm
900 MHz	29.65 nH	19 mm	1 mm	2 mm	6 mm	$46.4 + j0.0$
1800 MHz	No matching needed	18 mm	1 mm	2 mm	6 mm	$47.3 - j0.016$
<i>Model no. 2</i>						
Frequency	Matching lumped element	L_1	D_1	L_2	D_2	Impedance in ohm
900 MHz	25.24 nH	23 mm	1 mm	2 mm	6 mm	$42.2 + j0.0$
1800 MHz	No matching needed	22 mm	1 mm	2 mm	6 mm	$47.9 - j0.001$

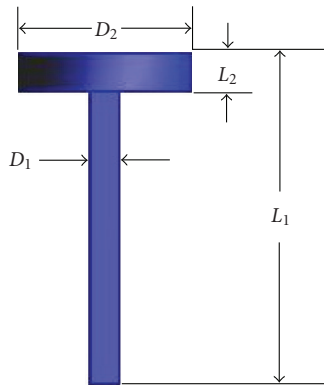


FIGURE 4: The proposed loaded short-whip antenna with dimensions.

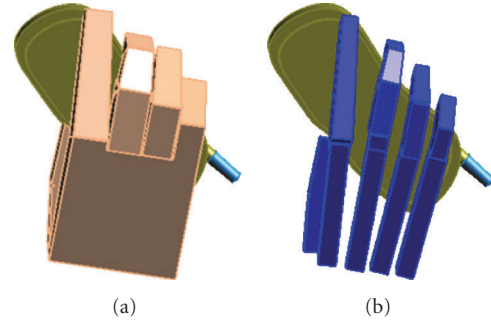


FIGURE 5: The CAD representation of the proposed semirealistic hand model holding the proposed handset; (a) all hand tissues, (b) hand-bones only.

model no. 2, the mesh cells amounts are 6.82675 Mcells and 4.89154 Mcells, at 900 MHz and 1800 MHz, respectively.

3.3. Cellular handset in hand close to head

As defined in IEEE standard 1528-2003 [7], two handset positions are considered in presence of human-head, *cheek* and *tilt* (15°). The head is simulated using both, homogeneous and nonhomogeneous phantoms.

The homogeneous head model is a SAM phantom available with [15] and consists of two dielectric materials, shell and liquid. The material parameters are defined in

[7, 8], with shell and ear spacer defined in [5], at 900 MHz and 1800 MHz.

The nonhomogeneous head phantom is a high-resolution European 40-year female head (HR-EFH), derived from MRI scan [15], and is imported to the *SEMCAD* platform. This CAD phantom consists of 121 different slices, with slice thicknesses of 1 mm (ear region) and 3 mm, and a transverse spatial resolution of 0.2 mm. The following different 25 tissues are recognized: *air, blood vessel, bones, brain/grey matter, brain/white matter, cerebellum, cerebrospinal fluid, ear (cartilage), eye-cornea, eye-lens, eye-vitreous body, fat, jaw, mastoid cells (bones), mid-brain,*

TABLE 2: The generated FDTD-grid properties of both handset models in hand close to head, SAM and HR-EFH.

Frequency	Handset	HR-EFH-Head phantom	
		Mesh cells amount/ <i>Cheek</i>	Mesh cells amount/ <i>Tilt</i>
900 MHz	Model no. 1	276*253*300 = 20.9484 Mcells	284*241*310 = 21.2176 Mcells
900 MHz	Model no. 2	290*251*281 = 20.4540 Mcells	282*239*305 = 20.5564 Mcells
1800 MHz	Model no. 1	268*244*288 = 18.8329 Mcells	276*233*302 = 19.4210 Mcells
1800 MHz	Model no. 2	289*242*277 = 19.3728 Mcells	274*231*296 = 18.7350 Mcells
Frequency	Handset	SAM-Head phantom	
		Mesh cells amount/ <i>Cheek</i>	Mesh cells amount/ <i>Tilt</i>
900 MHz	Model no. 1	208*135*234 = 6.57072 Mcells	208*131*252 = 6.86650 Mcells
900 MHz	Model no. 2	230*137*217 = 6.83767 Mcells	230*131*223 = 6.71899 Mcells
1800 MHz	Model no. 1	200*127*230 = 5.84200 Mcells	200*123*236 = 5.80560 Mcells
1800 MHz	Model no. 2	222*129*209 = 5.98534 Mcells	219*120*214 = 5.62392 Mcells

muscles, nasal cavity, parotid gland, spin, skull, spinal cord, spine, thalamus, tongue, and ventricles.

Head and hand tissues properties are set according to the material properties data-base in [15] and to that given in [18], where both are based on [19].

The FDTD-grid for each handset in hand close to head has a minimum spatial resolution of $0.5 \times 0.5 \times 0.5 \text{ mm}^3$ and maximum resolution of $10 \times 10 \times 10 \text{ mm}^3$ in the x , y , and z directions with grading ratio of 1.2. The absorbing boundary conditions (ABCs) are set as a perfectly matched layer (PML) mode with a very high-strength thickness [15].

Table 2 lists the amounts of mesh cells according to FDTD-grid setting for both handset models in hand close SAM and HR-EFH, at 900 MHz and 1800 MHz.

The simulations (in all cases) assume a steady-state voltage at the 900 and 1800 MHz, with a feed point of a 50-Ohm voltage source of 1-mm gap. A transient excitation of 12 periods is set as guarantee to achieving a steady state. The absorbing boundary conditions (ABCs) are set as a perfectly matched layer (PML) mode with a very high strength thickness [15].

In case of the handset close to head (both SAM and HR-EFH), the acoustic output referenced to earpiece is set according to IEEE standard 1528 [7]. Due to different antenna positions in both handset models, the distances between the antennas feed points and the nearest tissue voxel are different too. For the handset model no. 1 the acoustic output position is set at the origin, whereas for the handset model no. 2 the acoustic output position is set at ($x = -15$, $y = 0$ and $z = -104 \text{ mm}$). Figures 6(a) and 6(b) show both handset models close to head (SAM) at *cheek* position indicating the coordinate system, whereas Figure 6(c) shows the handset model no. 2 in hand close to head.

4. EM INTERACTION BETWEEN THE HANDSET ANATENNA AND HUMAN HEAD

The EM interaction between the handset antenna and human head is evaluated by; first, evaluating the effect of human head and hand on the handset antenna performance through computing the antenna parameters, including input

return loss, gain, radiation efficiency, and total efficiency, second, evaluating the impact of antenna EM radiation on the head through computing the induced SAR and power absorption.

4.1. Antenna performance

Table 3 demonstrates the antenna parameters including; input return loss, gain, radiation efficiency, and total efficiency, for both handset models in all cases at 900 MHz. Table 4 lists the antenna parameters at 1800 MHz. Figure 7 shows the radiation beam pattern in (V/m) for both handset models in hand close to HR-EFH at *cheek* position and for both 900 and 1800 MHz frequencies, whereas Figure 8 shows the radiation beam pattern at *tilt* position.

4.2. SAR and power loss computation in head

The impact of the electromagnetic (EM) wave irradiation on the living body is measured by evaluating the SAR which is defined as the amount of EM energy absorption in the unit mass as follow [20]:

$$\text{SAR} = \frac{\sigma_E}{\rho} |\mathbf{E}|^2, \quad (1)$$

where σ_E (S/M) is the conductivity, \mathbf{E} (V/m) is the the induced electric field vector, and ρ (kg/m^3) is the material density. Using SEMCAD platform, an algorithm based on SCC34/SC2/WG2 computational dosimetry, IEEE-1529 [21], the spatial peak SAR can be computed over any required mass.

The spatial-peak SAR should be evaluated in a cubical volume of the body tissues that is within 5% of the required mass [15]. The averaged peak-SAR (Spatial-peak SAR [IEEE-1529]) can be specified over a cube of 1g and 10g mass, and normalized to a certain source power. Referred to the IEEE standard C95.1b-2004 [22] (for low-power devices, uncontrolled environment), the antenna input power is set to 0.6 W at 900 MHz and 0.125 W at 1800 MHz, respectively, in all cases.

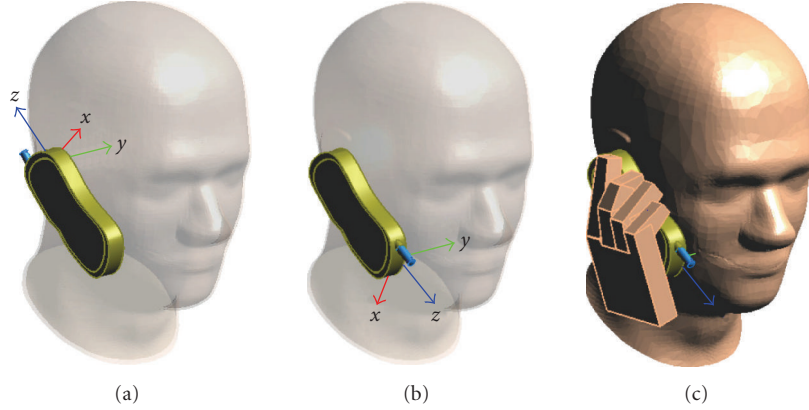


FIGURE 6: Coordinate system; (a) the handset model no. 1 referenced as seen from the right side of the SAM, at *cheek* position, (b) the handset model no. 2 referenced as seen from the right side of the SAM, at *cheek* position, and (c) the handset model no. 2 in hand close to SAM at *cheek* position.

TABLE 3: Computational results of the antenna performance parameters of both handset models at 900 MHz in all cases.

Frequency	900 MHz							
	$ S_{11} $ in (dB)		Gain (dBi)		Radiation efficiency		Total efficiency	
	Model no. 1	Model no. 2	Model no. 1	Model no. 2	Model no. 1	Model no. 2	Model no. 1	Model no. 2
Handset in free-space	-28.4	-21.5	1.72	1.8	85.76%	86.9%	85.63%	86.33%
Handset in hand only	-12.9	-15.4	1.23	-0.6	48.4%	41.0%	45.9%	39.7%
Handset in hand close to SAM (<i>Cheek</i> position)	-15.4	-17.5	-5.98	-5.86	7.3%	11.7%	7.1%	11.5%
Handset in hand close to SAM (<i>Tilt</i> position)	-17.3	-18.2	-2.75	-2.5	18.8%	21.5%	18.5%	21.2%
Handset in hand close to HR-EFH (<i>Cheek</i> position)	-13.8	-24.2	-5.5	-3.5	12.8%	17.3%	12.3%	17.2%
Handset in hand close to HR-EFH (<i>Tilt</i> position)	-17	-19	-2.8	-2.1	25.0%	25.6%	24.5%	25.3%

Table 5 lists the computed peak SAR averaged over 1g and 10g, and the absorbed power in tissues, for both handset models at both positions and at 900 MHz. Table 6 lists the computed parameters at 1800 MHz.

Figure 9 shows the sliced-distribution of the averaged peak SAR_{1g} in the HR-EFH phantom exposed to EM radiation of both model no. 1 and model no. 2 antennas at *cheek* position and at different frequencies, whereas Figure 10 shows the sliced-distribution of the averaged peak SAR_{1g} in the HR-EFH phantom exposed to EM radiation at *tilt* position.

5. TOTAL ISOTROPIC SENSITIVITY

The total isotropic sensitivity (TIS) [15] is a measure of the handset receiving performance. The TIS and TRP (total radiated power) together determine effectiveness of the handset as a piece of radio equipment, in particular the maximum range at which the handset can operate from the base station with some given level of performance [23]. The computed TIS for both handset models at 900 MHz and 1800 MHz are given in Tables 5 and 6.

6. COMPUTATION ERROR

The computation error is defined as [24]

$$\text{Computation error} = |P_{\text{in}} - (P_{\text{rad}} + P_{\text{abs}} + P_{\text{Loss}})| / P_{\text{in}},$$

$$P_{\text{Loss}} = P_d + P_c, \quad (2)$$

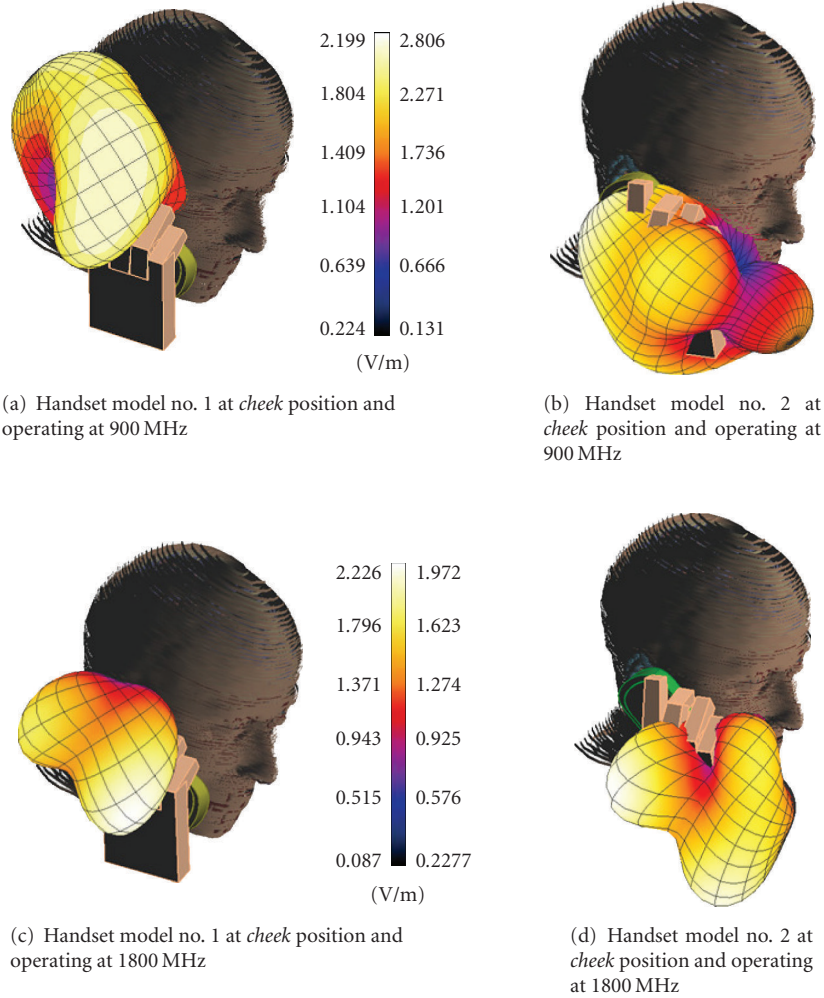
where P_{in} is the input power, P_{rad} is the radiation power, P_{abs} is the absorbed power in tissues, and P_{Loss} is the total power loss. P_{Loss} includes the dielectric loss (P_d) and the metallic ohmic loss (P_c).

7. DISCUSSION

The results in Tables 3 and 4 reveal that presence of a head close to the handheld set of model no. 1 degrades the handset performance, significantly reducing the handset total efficiency to about (8%–28%) of the total efficiency of the handset in free space. Adopting a bottom-mounted antenna, model no. 2, the total efficiency of the handset model no. 1 can be improved by (3.3%–45.5%), whereas the

TABLE 4: Computational results of the antenna performance parameters of both handset models at 1800 MHz in all cases.

Frequency	1800 MHz							
	$ S_{11} $ in (dB)		Gain (dBi)		Radiation efficiency		Total efficiency	
	Model no. 1	Model no. 2	Model no. 1	Model no. 2	Model no. 1	Model no. 2	Model no. 1	Model no. 2
Handset in free-space	-31.2	-33.4	3.9	3.8	95.3%	95.8%	95.2%	95.7%
Handset in hand only	-19	-17.2	2.9	0.86	67.1%	50.0%	66.2%	49.0%
Handset in hand close to SAM (<i>Cheek</i> position)	-17.8	-22.8	0.2	-0.15	22.3%	30.1%	22%	30.0%
Handset in hand close to SAM (<i>Tilt</i> position)	-15.4	-21	0.67	0.86	26.1%	36.7%	25.0%	36.4%
Handset in hand close to HR-EFH (<i>Cheek</i> position)	-17.1	-21	1.3	0.2	25.0%	33.4%	24.5%	33.1%
Handset in hand close to HR-EFH (<i>Tilt</i> position)	-16.5	-19.2	0.6	0.47	27.2%	39.2%	26.6%	38.7%

FIGURE 7: The three-dimensional radiation pattern in (V/m) of both handset models in hand close to HR-EFH at *cheek* position and operating at different frequencies.

gain is reduced by (0.19–2.15 dBi). The antennas of both handset models were matched well for all the cases.

Since the proposed handset model has an antenna in a low-noise area of the handset and well separated from the potentially noisy components, it has the potential to achieve better TIS. According to the results obtained in Tables 5 and

6, the different cases of the handset model no. 2 in hand close to head do show better TIS values, as compared with model no. 1, due to the improved total efficiency.

Moreover, Tables 5 and 6 show that the averaged peak-SAR_{1g} induced in head close to hand-held of model no. 1 can be reduced by (28%–92.2%) using the proposed handset

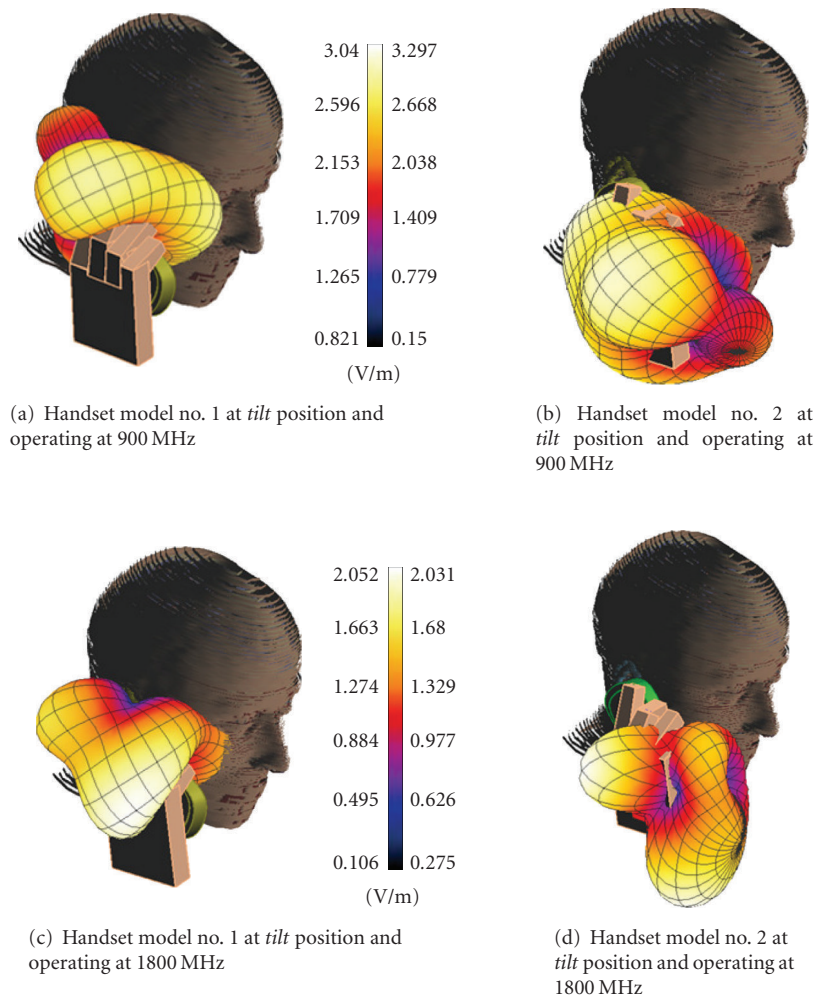


FIGURE 8: The three-dimensional radiation pattern in (V/m) of both handset models in hand close to HR-EFH at *tilt* position and operating at different frequencies.

TABLE 5: The computed averaged peak-SAR (over 1g and 10g) and power absorption in tissues, radiated power, total loss, total isotropic sensitivity, and computation error for both handset models in hand close to head at different positions and at 900 MHz.

Handset model	900 MHz- <i>Cheek</i>				900 MHz- <i>Tilt</i>			
	SAM		HR-EFH (Adult)		SAM		HR-EFH (Adult)	
	Model no. 1	Model no. 2	Model no. 1	Model no. 2	Model no. 1	Model no. 2	Model no. 1	Model no. 2
Input power (mW)	600	600	600	600	600	600	600	600
Peak-SAR _{1g} (W/Kg) in head	4.23	3.34	2.99	2.72	1.86	1.34	4.17	1.09
Peak-SAR _{10g} (W/Kg) in head	3.02	2.38	2.55	2.27	1.29	0.98	1.40	0.92
Peak-SAR _{1g} (W/Kg) in hand	1.44	2.70	1.69	2.93	2.02	3.54	2.18	3.57
Peak-SAR _{10g} (W/Kg) in hand	0.82	1.25	0.89	1.31	1.18	1.65	1.19	1.65
Radiated power (mW)	42.60	69.00	74.00	103.50	127.20	110.10	147.00	152.00
Absorbed power in head (mW)	335.20	241.40	312.00	218.50	206.80	126.60	206.00	122.00
Absorption rate in head (%)	55.87	40.23	52.00	36.42	34.47	21.10	34.33	20.33
Absorbed power in hand (mW)	92.27	161.50	94.30	167.90	133.20	224.80	130.00	207.00
Total loss (mW)	103.26	107.20	109.00	99.83	106.20	115.50	108.70	110.00
Total isotropic sensitivity (dBm)	-94.5	-96.6	-97	-98.4	-99.3	-98.7	-99.9	-100.1
Computation error (%)	4.4	3.5	1.8	1.7	4.8	2.9	0.8	1.6

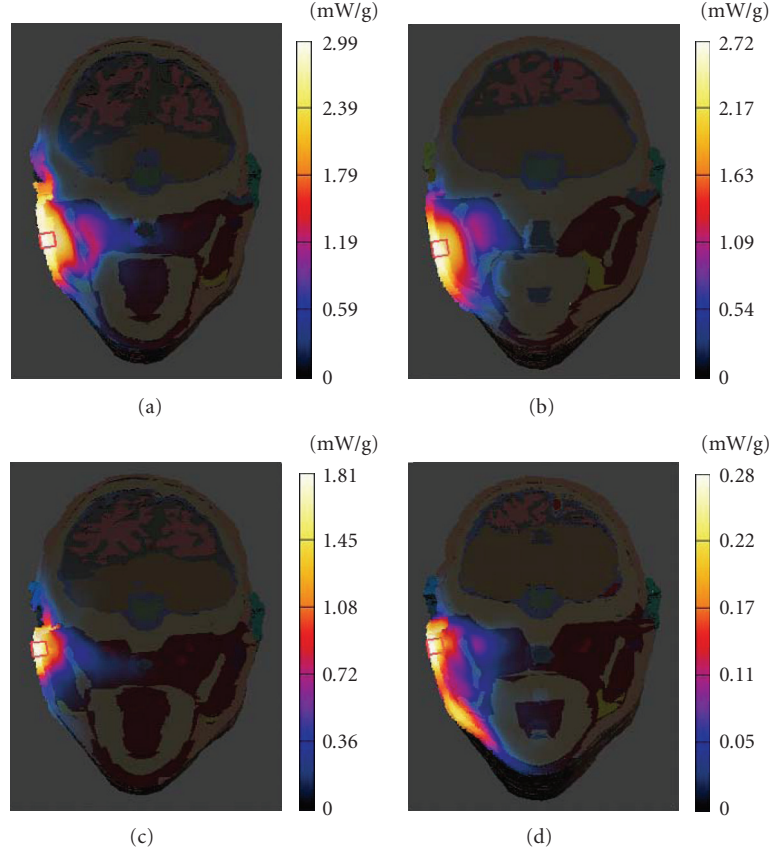


FIGURE 9: Sliced-distribution of the averaged peak SAR_{1g} in the yz -plane of the HR-EFH phantom in cases of handset models at *cheek* position. The antenna input powers are 0.6 W and 0.125 W for the frequencies 900 MHz and 1800 MHz, respectively. (a) Model no. 1 at 900 MHz, (b) Model no. 2 at 900 MHz, (c) Model no. 1 at 1800 MHz, (d) Model no. 2 at 1800 MHz.

TABLE 6: The computed averaged peak-SAR (over 1g and 10g) and power absorption in tissues, radiated power, total loss, total isotropic sensitivity, and computation error for both handset models in hand close to head at different positions and at 1800 MHz.

Handset model	1800 MHz- <i>Cheek</i>				1800 MHz- <i>Tilt</i>			
	SAM		HR-EFH (Adult)		SAM		HR-EFH (Adult)	
	Model no. 1	Model no. 2	Model no. 1	Model no. 2	Model no. 1	Model no. 2	Model no. 1	Model no. 2
Input power (mW)	125	125	125	125	125	125	125	125
Peak- SAR_{1g} (W/Kg) in head	1.38	0.47	1.81	0.28	1.29	0.14	1.93	0.15
Peak- SAR_{10g} (W/Kg) in head	0.87	0.30	1.13	0.18	0.82	0.08	0.97	0.10
Peak- SAR_{1g} (W/Kg) in hand	0.73	1.22	0.73	1.25	0.80	1.47	0.80	1.43
Peak- SAR_{10g} (W/Kg) in hand	0.42	0.64	0.42	0.66	0.45	0.71	0.46	0.73
Radiated power (mW)	27.50	37.45	30.65	41.40	31.67	45.55	33.34	48.40
Absorbed power in head (mW)	59.50	25.46	61.00	21.50	51.18	12.39	54.20	12.16
Absorption rate in head (%)	47.60	20.37	48.80	17.20	40.94	9.91	43.36	9.73
Absorbed power in hand (mW)	24.40	51.28	24.97	52.30	29.00	55.20	29.55	55.57
Total loss (mW)	7.66	7.21	7.43	7.80	7.66	7.84	7.19	7.65
Total isotropic sensitivity (dBm)	-98.8	-100.8	-100	-101.3	-100.1	-101.6	-100.3	-101.9
Computation error (%)	4.4	3.8	1.4	1.5	4.4	3.2	0.6	1.0

model no. 2, and the power absorbed in head can also be reduced by (27.9%–77.5%). The computation errors are less than 2% for all cases in presence of HR-EFH, whereas for the cases of SAM presence they are (1.4%–4.4%).

The differences in the induced SAR and absorption power values in both SAM and HR-EFH phantoms are due

to their different masses, volumes, and densities distribution. According to simulation results, HR-EFH mass is approximately 4.71 kg and the volume is approximately 4118 cm³, while the SAM mass is approximately 6.024 kg (considering a homogeneous density of 1000 kg/m³) and the volume is approximately 6043 cm³.

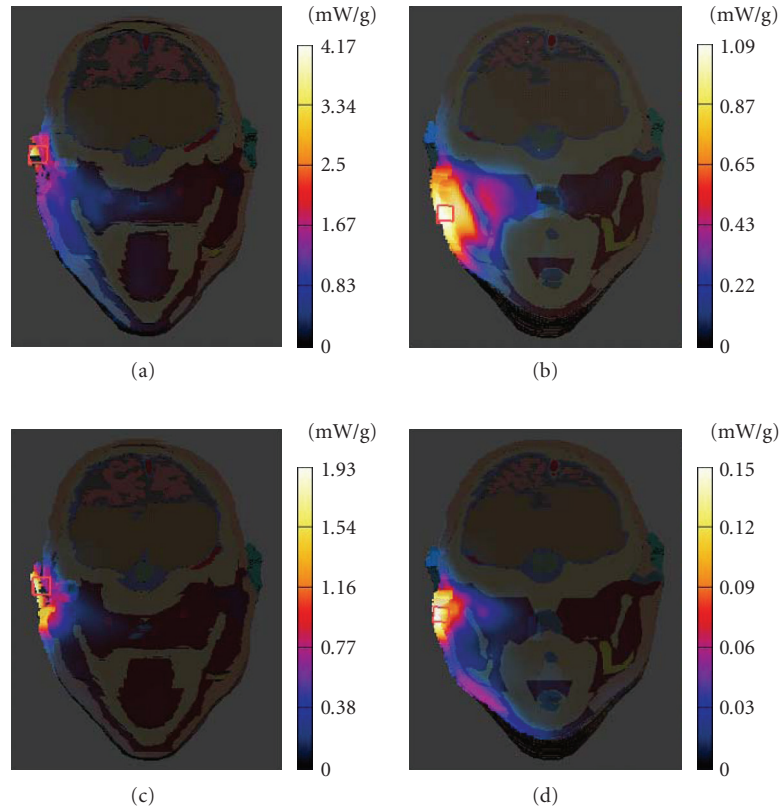


FIGURE 10: Sliced-distribution of the averaged peak SAR_{1g} in the yz -plane of the HR-EFH phantom in cases of handset models at *tilt* position. The antenna input powers are 0.6 W and 0.125 W for the frequencies 900 MHz and 1800 MHz, respectively. (a) Model no. 1 at 900 MHz, (b) Model no. 2 at 900 MHz, (c) Model no. 1 at 1800 MHz, (d) Model no. 2 at 1800 MHz.

The proposed human-hand model mass is approximately 0.248 kg and its volume is approximately 186 cm^3 .

All computations are performed on a 2.0-GHz Intel centrino Laptop machine (Dell, inspiron-630 m) with 2 GB memory (dual-channel technology), and operating under MS Windows-vista. The runtime and memory requirements depend on the simulation space. Less memory and runtime are required for the handset simulation in free space, whereas, more memory and runtime are required for the handset in hand close to head. The machine-memory is enough to achieve all simulations with the mesh cells amounts listed in Table 2. The runtimes are about 1–10 hours.

8. CONCLUSION

A cellular handset with a keypad over the screen and a bottom-mounted antenna has been proposed and numerically modeled, with the most handset components, using an FDTD-based *SEMCAD* platform. The proposed handset model is based on the commercially available model with a top-mounted external antenna. Both homogeneous and nonhomogeneous head phantoms have been used with a semirealistic hand design to simulate the handset in hand close to head. The simulation results showed a significant improvement in the antenna performance with the proposed

handset model in hand close to head, as compared with the handset of top-mounted antenna. Also, using this proposed handset, a significant reduction in the induced SAR and power absorbed in head has been achieved.

REFERENCES

- [1] N. K. Kouveliouis, S. C. Pabagiotou, P. K. Varlamos, and C. N. Capsalis, "Theoretical approach of the interaction between a human head model and a mobile handset helical antenna using numerical methods," *Progress in Electromagnetics Research*, vol. 65, pp. 309–327, 2006.
- [2] K. Sulonen and P. Vainikainen, "Performance of mobile phone antennas including effect of environment using two methods," *IEEE Transaction on Instrumentation and Measurement*, vol. 52, no. 6, pp. 1859–1864, 2003.
- [3] J. Krogerus, C. Icheln, and P. Vainikainen, "Dependence of mean effective gain of mobile terminal antennas on side of head," in *Proceedings of the 35th European Microwave Conference*, pp. 467–470, Paris, France, October 2005.
- [4] H. Haider, H. Garn, G. Neubauer, and G. Schmidt, "Investigation of mobile phone antennas with regard to power efficiency and radiation safety," in *Proceedings of the Workshop on Mobile Terminal and Human Body Interaction*, Bergen, Norway, April 2000.
- [5] B. B. Beard, W. Kainz, T. Onishi, et al., "Comparisons of computed mobile phone induced SAR in the SAM phantom to that in anatomically correct models of the human head," *IEEE*

- Transaction on Electromagnetic Compatibility*, vol. 48, no. 2, pp. 397–407, 2006.
- [6] N. Chavannes, R. Tay, N. Nikoloski, and N. Kuster, “Suitability of FDTD-based TCAD tools for RF design of mobile phones,” *IEEE Antennas and Propagation Magazine*, vol. 45, no. 6, pp. 52–66, 2003.
- [7] “Recommended Practice for Determining the Peak Spatial-Average Specific Absorption Rate (SAR) in the Human Head from Wireless Communications Devices—Measurement Techniques,” IEEE Standard-1528, December 2003.
- [8] “Human Exposure to Radio Frequency Fields from Hand-Held and Body-Mounted Wireless Communication Devices—Human Models, Instrumentation, and Procedures—Part 1: Procedure to Determine the Specific Absorption Rate (SAR) for Hand-Held Devices Used in Close Proximity to the Ear (Frequency Range of 300 MHz to 3 GHz),” IEC 62209-1, 2005.
- [9] “Basic Standard for the Measurement of Specific Absorption Rate Related to Exposure to Electromagnetic Fields from Mobile Phones (300 MHz–3 GHz),” European Committee for Electrical Standardization (CENELEC), EN 50361, 2001.
- [10] “Specific Absorption Rate (SAR) Estimation for Cellular Phone,” Association of Radio Industries and Businesses (ARIB) STD-T56, 2002.
- [11] “Federal Communications Commission (FCC) Evaluating Compliance with FCC Guidelines for Human Exposure to Radio Frequency Electromagnetic Fields,” Supplement C to OET Bulletin 65 (Edition 9701), Washington, DC: FCC, 1997.
- [12] J. Wang and O. Fujiwara, “Comparison and evaluation electromagnetic absorption characteristics in realistic human head models of adult and children for 900 MHz mobile telephones,” *IEEE Transaction on Microwave Theory and Techniques*, vol. 51, no. 3, pp. 966–971, 2003.
- [13] J. Wang, O. Fujiwara, and S. Watanabe, “Approximation of aging effect on dielectric tissue properties for SAR assessment of mobile telephones,” *IEEE Transaction on Electromagnetic Compatibility*, vol. 48, no. 2, pp. 408–413, 2006.
- [14] M. Burkhardt, “Contributions toward uncertainty assessments and error minimization of FDTD simulations involving complex dielectric bodies,” Ph.D. dissertation, Diss. ETH Nr.13176, Zurich, Switzerland, 1999.
- [15] SEMCAD, Reference Manual for the SEMCAD Simulation Platform for Electromagnetic Compatibility, Antenna Design and Dosimetry, SPEAG-Schmid & Partner Engineering AG, <http://www.semcad.com/>.
- [16] <http://www.linuxdevices.com/news/NS7002110505.html>.
- [17] K. Ogawa and T. Uwano, “A diversity antenna for very small 800 MHz band portable telephones,” *IEEE Transaction on Antenna and Propagation*, vol. 42, no. 9, pp. 1342–1345, 1994.
- [18] Dielectric Properties of Body Tissue in the frequency range 10 Hz–100 GHz Italian National Research Council, Institute for Applied Physics, Florence, Italy, <http://niremf.ifac.cnr.it/tissprop/>.
- [19] C. Gabriel, “Compilation of the dielectric properties of body tissues at RF and microwave frequencies,” Tech. Rep. N.AL/OE-TR-1996-0037, Occupational and Environmental Health Directorate, Radiofrequency Radiation Division, Brooks Air Force Base, San Antonio, Tex, USA, June 1996.
- [20] H. Arai, *Measurement of Mobile Antenna Systems*, Artech House, Norwood, Mass, USA, 2001.
- [21] “Recommended Practice for Determining the Peak Spatial-Average Specific Absorption Rate (SAR) associated with the use of wireless handsets—computational techniques,” draft standard, IEEE-1529.
- [22] “IEEE Standard for safety Levels with respect to human exposure to radio frequency electromagnetic fields, 3 kHz to 300 GHz, Amendment 2: Specific Absorption Rate (SAR) Limits for the Pinna,” IEEE Standard C95.1b-2004, December 2004.
- [23] Z. N. Chen, *Antennas for Portable Devices*, John Wiley & Sons, Hoboken, NJ, USA, 2007.
- [24] L. C. Kuo, Y. C. Kan, and H. R. Chuang, “Analysis of a 900/1800 MHz dual-band gap loop antenna on a handset with proximate head and hand model,” *Journal of Electromagnetic Waves and Applications*, vol. 21, no. 1, pp. 107–122, 2007.



Hindawi

Submit your manuscripts at
<http://www.hindawi.com>

